Optics Letters

Femtosecond laser one-step direct-writing cylindrical microlens array on fused silica

Zhi Luo,[1] Ji'an Duan,[2] and Chunlei Guo[1,3,*]

[1]The Institute of Optics, University of Rochester, Rochester, New York 14627, USA
[2]The State Key Laboratory of High Performance and Complex Manufacturing, Central South University, Changsha 410083, China
[3]The Guo China-U.S. Photonics Lab, Changchun Institute of Optics, Fine mechanics, and Physics, Changchun 130033, China
*Corresponding author: guo@optics.rochester.edu

Received 27 April 2017; revised 24 May 2017; accepted 24 May 2017; posted 25 May 2017 (Doc. ID 294603); published 13 June 2017

We demonstrate an efficient method for fabricating high-quality cylindrical microlens arrays (CMLAs) on the surface of fused silica, fully based on spatially shaping of a femtosecond laser beam from Gaussian to Bessel distribution. As the envelope of shaped spatial intensity distribution matches the profile of cylindrical microlens perfectly, a CMLA with more than 50 uniform microlenses is fabricated by simple line scanning. The radius and height of these microlens units can be finely controlled by adjusting the power of laser pulses. Excellent optical imaging and high-speed fabrication performances are also demonstrated by our fabricated CLMA.

OCIS codes: (320.2250) Femtosecond phenomena; (320.5540) Pulse shaping; (220.4000) Microstructure fabrication.

https://doi.org/10.1364/OL.42.002358

Microlens arrays, referring to an array of small lenses uniformly distributed on the surface of substrates with diameters varying from several micrometers to nearly a millimeter [1,2], have various applications such as photovoltaic devices, micro-optical systems, artificial compound eyes, and artificial compound eyes [3,4]. Currently, there are many methods to fabricating microlens arrays over a large area with a controllable curvature, such as hot embossing [5], laser direct writing [6], and digital projection photopolymerization [7]. However, these methods are usually only suitable for producing a spherical lens array due to their simple symmetrical shapes.

Producing nonspherical cylindrical microlens arrays (CMLAs) poses a greater challenge. In industry, reflow or resist-melting techniques are usually used to produce CMLAs [8,9]. Although these techniques can fabricate large microlens arrays with good optical quality, their manufacturing processes are very complicated, including multiple steps such as resist coating, photolithography, wet process, etc., and all process parameters have to be carefully optimized. Besides, the profile of fabricated microlenses is usually deformed by reactive ion etching.

Laser-assisted fabrication can provide an alternative way for material micro-processing [10,11]. Shao *et al.* proposed a laser-assisted polymer swelling method for the fabrication of microlens arrays with a large curvature [12]. Choi *et al.* fabricated a plano–convex CMLA on a fused silica surface with multiple laser processing methods, including a femtosecond (fs) laser processing followed by CO_2 laser reshaping [13]. These methods usually involve multistep complex processing techniques. In addition, the efficiency of these methods is usually low when fabricating a CMLA over a large area. To meet the requirement of their extensive applications, a simple, fast, cost-effective, and well-controlled approach to fabricate large-area and high-quality CMLA is needed.

Typically, a Gaussian beam can be transformed to a Bessel beam by an axicon lens [14–16]. However, the transformed beam is usually very weak and cannot be used for material processing. To increase the Bessel beam intensity, it requires a precise 4f focusing system. In this Letter, we have obtained a true Bessel beam by utilizing a 4f focusing optical setup. As a result, the beam quality is high, and the intensity is significantly enhanced, allowing us to process hard materials such as fused silica which has a wide range of applications in the field of optics. Based on the shaped Bessel beam, a high-quality CMLA is fabricated on the fused silica by simply line scanning. The profile of these mirolens units has a perfect semi-circular shape, and the radius can be finely controlled. Moreover, the result shows excellent optical imaging performance after simply being polished with cerium dioxide (CeO_2).

During fs laser fabricating, the microstructures engraved on the surface of target material with different morphologies can be attributed to different focusing geometry of laser beam. In other words, the profile of processed microstructures depends on the envelope of laser spatial intensity distribution. The Bessel beam is termed a diffraction-free beam because the transverse profile of the beam remains unaltered during free-space propagation [17]. It has received increasing attention for ultrafast laser applications in recent years [14]. In this Letter, we will show that fs laser pulses with Bessel beam profiles can be very efficient in cutting cylindrical microstructures from the surface of a sample. To understand the formation of cylindrical microlenses, we first perform numerical simulations to compare the spatial intensity distribution between a Bessel beam and a Gaussian beam. Based on mathematical models [15,16], the spatial intensity profiles of an axicon-formed Bessel beam, and

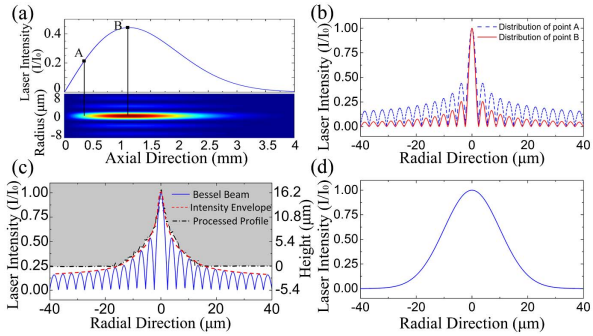

Fig. 1. Laser intensity profile of a Bessel beam in (a) the axial direction, and (b) and (c) the radial direction. (d) Gaussian beam spatial intensity distribution.

a Gaussian beam can be depicted as Fig. 1. The central laser intensity distribution of the Bessel beam in the axial direction is shown in Fig. 1(a). For the focal plane in which the peak point B is located, the laser intensity is mainly gathered in the central lobe, as characterized by the solid line in Fig. 1(b). If such a focal plane is located on the sample surface to fabricate microstructures, the laser intensity of the side lobes is too low to ablate material. The uniqueness of an axicon-formed Bessel beam is that the intensity profile, i.e., the intensity balancing between the central peak versus the side lobes, can be varied at different planes off focus, and this allows us to match the profile of cylindrical microlenses with a Bessel beam plane. For example, the intensity of side lobes can be amplified by defocusing the beam front from the peak point B to point A, as shown in Fig. 1(a). Because the total energy of incident laser is constant, the profile of the intensity distribution will be transformed to the shape of the dashed line in Fig. 1(b). Figure 1(c) shows the envelope of the shaped intensity distribution that perfectly matches the profile of two adjacent quarter-cylinders. The linearity remains a valid fit in the fluence range in our experiments. Figure 1(d) shows the spatial intensity distribution of a TEM_{00} Gaussian beam, and its profile is similar to an approximately equilateral triangle. In contrast to a Bessel beam, the intensity ration of a Gaussian beam between the center and the edge cannot be varied at different propagation planes, thus un-suitable to produce a desired intensity profile as by a Bessel beam.

For the setup used to fabricate CMLA, the laser source is a Ti:sapphire amplified fs laser system. The beam produced has a central wavelength of 800 nm, pulse duration of 65 fs, and a repetition rate of 1 kHz. After being set with expected parameters, the laser beam is transformed into a Bessel beam by an axicon lens, and a 4f lens system is used to compress the size of the beam and to increase the laser intensity at the focal spot. A re-collimated Bessel beam is created with the central radius of about 112 μm and the depth of focus of about 960 μm. The conical angle of the axicon is 2.5°. The 4f system is made up of a bi-convex lens and a plano–convex lens, whose focal lengths are 300 and 25.4 mm, respectively. The final Bessel beam is focused on the front surface of samples (fused silica), and the experimentally measured ablation threshold fluence is about 1.38 J/cm^2. During the CMLA fabrication experiment, the sample moves along one axis on the beam perpendicular plane at a constant velocity to engrave grooves and moves along another axis by a constant distance after each processed groove. As a comparison experiment, we also directly guide the original output Gaussian beam to ablate the sample. After irradiation with the shaped Bessel beam and the original Gaussian beam, a confocal laser scanning microscope and an optical microscope are used to characterize fabricated microstructures.

Experimentally, a cylindrical microlens can be formed by placing two scanning laser lines together, each giving a quarter-cylinder profile. A quarter-cylinder will have a height-to-width ratio, aspect ratio, of 1. The laser power and writing speed also play a role in affecting the aspect ratio. We measure the dependence of the aspect ratio as a function of the laser power and writing speed, respectively. We find that a laser power of 500 mW (the average pulse fluence of about 1.27 J/cm^2 and below the air breakdown threshold) and a writing speed of 0.4 mm/s give an aspect ratio close to 1. The overlap ratio of two adjacent pulses is more than 99% with such a speed. We determine that a defocus distance of 0.6 mm gives us an excellent spherical shape and, thus, we will produce a CMLA with these laser parameters.

Figure 2(a) shows a line fabricated by direct laser writing with a spatially shaped fs laser Bessel beam. We can see that the line profile, as shown in Fig. 2(b), shows an excellent agreement with the intensity envelope in Fig. 1(c). As a comparison, the original Gaussian beam from the laser amplifier system, is also used to ablate the fused silica surface after passing through a lens. (The focal length is 25.4 mm.) The same scanning speed and defocus distance are used for the Gaussian beam, while the power of 100 mW is used for the Gaussian beam to produce a similar level of surface structures. The ablated result is shown in Fig. 2(c). As shown in Fig. 2(d), the profile of microstructure processed by the Gaussian beam is close to a triangle, which is significantly different from the result with a Bessel beam, but shows an excellent agreement to the theoretical simulations,

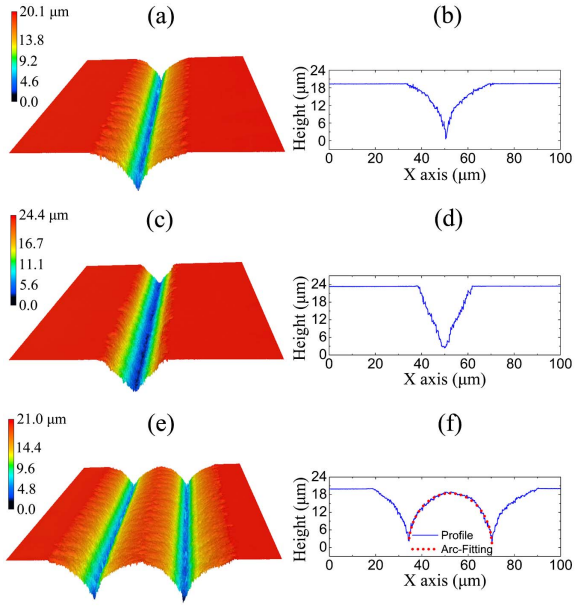

Fig. 2. Microstructures processed on the surface of fused silica by a fs laser with different spatial intensity distribution: (a) Bessel beam and (c) Gaussian beam. Image (e) is formed by a seamless combination of two microstructures of Image (a). Images (b), (d), and (f) are the corresponding cross-sectional profiles.

as shown in Fig. 1(d). As mentioned earlier, the 4f focusing is also critical to achieve a higher intensity, while preserving the Bessel beam. This can be seen from a previous work in [18], where two random focusing lenses were used to focus a Bessel beam to increase its intensity. In that study, the focused beam became a ring-like focusing structure, and the final focus was not a Bessel beam anymore. As a result, the study in [18] showed a poor focus quality, low intensity, and could only process very soft materials, such as polymethyl methacrylate (PMMA). When the fabrication of CMLA was attempted, the produced structure was irregular, and the fabricated lens array does not have the type of optical performance, as shown later in this Letter. Therefore, we conclude that the spatial intensity distribution plays a critical role in forming different surface profiles for fs laser fabricating microstructures. Furthermore, the most significant benefit of the Bessel beam processed microstructures is that by placing two adjacent to each other, a cylindrical microlens is produced between, as shown in Fig. 2(e). The cross-sectional profile of the cylindrical microlens is approximate to a semicircle, and a semicircle function is adopted to fit the central profile curve by using ORIGINPRO. After performed 16 iterations, the fitting curve converges to match the profile curve perfectly, as shown in Fig. 2(f). The fitting factor reaches 0.985. (1 is the ideal situation.) The diameter of the fitting curve is 17.99 μm, which is in good agreement with the designed size of 18 μm.

Applying the approach as described above, a CMLA can be fabricated by fs laser direct-writing, as shown in Fig. 3. The designed length and cycle number of the CMLA are 3 mm and 50, respectively. Additionally, the height (radius) of the cylindrical microlens unit can be controlled to range from several micrometers to about 30 μm by using different laser powers. It is found that the height (radius) of the cylindrical microlens varies almost linearly with laser power, as shown in Fig. 3(c), and the slope of the fitting line is about 0.02 μm/mW. Figures 3(a) and 3(b) show the CMLAs with different heights (9.02 and 17.99 μm, respectively). In addition, the two insets are the partial enlarged views of the corresponding results.

To demonstrate the optical imaging performances of CMLAs, several focusing experiments are carried out. First, a CMLA was positioned vertically on a sample stage and moved relative to the objective lens. The CMLA was illuminated with a white light from behind, as shown in Fig. 4(a). Then, on the focal plane of the CMLA, an array of bright lines could be

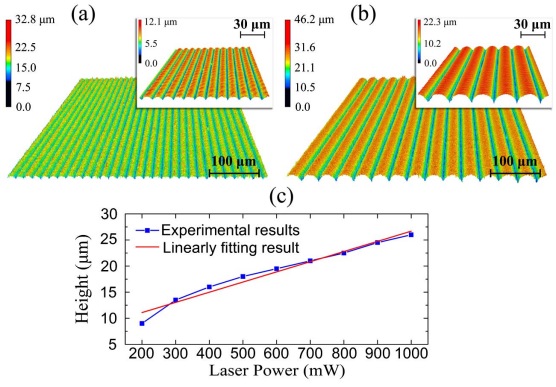

Fig. 3. CMLA with different heights and radii of (a) 9 μm and (b) 18 μm. (c) Linear relationship between the height and laser power.

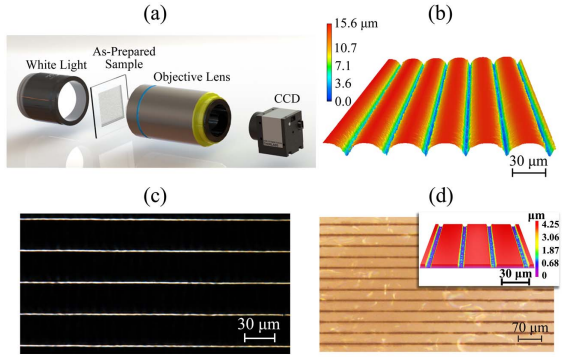

Fig. 4. Polishing results with CeO_2 and their focusing performance. (a) Illustration of experimental setup, (b) fabricated CMLA, (c) focusing results with the CMLA, and (d) a grating directly fabricated by using an as-prepared CMLA.

observed through a CCD camera. The focusing performance of the CMLAs we produced is very high and can be further improved by polishing with CeO_2 particles. Figure 4(b) shows the fabricated CMLA, and Fig. 4(c) shows that the focused line intensity is essentially constant along both X and Y axes, which indicates that the fabricated CMLAs are consistent in size and profile throughout the processing area.

The high quality of the CMLAs we produced allows us to perform high-speed material processing by focusing a laser beam to parallel line focusing. To demonstrate this, we use an as-prepared CMLA to focus a fs laser beam to a line focusing, as shown in Fig. 4(c). A low-ablation-threshold PMMA is placed at the line focusing plane, and an excellent reproduction of the line focusing can be seen following the ablation experiments, as shown in Fig. 4(d). The inset is a partial enlarged 3D view. We can see that a micro-grating structure is formed on the sample surface with only several laser pulses and without any movement of the laser beam or the sample. Therefore, our CMLAs have a potential to produce high-quality gratings.

In this Letter, we demonstrate an efficient way for fabricating high-quality CMLAs on the surface of fused silica, fully based on fs laser beam shaping. The laser intensity distribution is transformed from a Gaussian to a Bessel profile. Numerical simulations demonstrate that the envelope of the shaped intensity distribution matches perfectly to the profile of the cylindrical microlens. A CMLA is fabricated on fused silica by simply line scanning a shaped fs laser line by line. The radius and depth of these microlens units can be controlled in the range of several micrometers to over 30 μm by adjusting the power of laser pulses. Finally, excellent optical imaging and high-speed fabrication performances are demonstrated by our fabricated CLMA.

Funding. Army Research Office (ARO); Bill and Melinda Gates Foundation; China Scholarship Council (CSC).

REFERENCES

1. H. Yabu and M. Shimomura, Langmuir **21**, 1709 (2005).
2. A. Y. Yi and L. Li, Opt. Lett. **30**, 1707 (2005).
3. P. Dannberg, F. Wippermann, A. Brückner, A. Matthes, P. Schreiber, and A. Bräuer, Micromachines **5**, 325 (2014).

4. Z. Deng, F. Chen, Q. Yang, H. Bian, G. Du, J. Yong, C. Shan, and X. Hou, Adv. Funct. Mater. **26**, 1995 (2016).
5. C. Y. Chang and C. H. Yu, J. Micromech. Microeng. **25**, 025010 (2015).
6. J. Yong, F. Chen, Q. Yang, G. Du, H. Bian, D. Zhang, J. Si, F. Yun, and X. Hou, ACS Appl. Mater. Interfaces **5**, 9382 (2013).
7. Y. Lu and S. Chen, Appl. Phys. Lett. **92**, 041109 (2008).
8. P. Nussbaum, R. Voelkel, H. P. Herzig, M. Eisner, and S. Haselbeck, Pure Appl. Opt. **6**, 617 (1997).
9. H. Ottevaere, R. Cox, H. P. Herzig, T. Miyashita, K. Naessens, M. Taghizadeh, R. Völkel, H. J. Woo, and H. Thienpont, J. Opt. A **8**, S407 (2006).
10. A. Y. Vorobyev and C. Guo, Laser Photon. Rev. **7**, 385 (2013).
11. Y. L. Zhang, Q. D. Chen, H. Xia, and H. B. Sun, Nano Today **5**, 435 (2010).
12. J. Shao, Y. Ding, H. Zhai, B. Hu, X. Li, and H. Tian, Opt. Lett. **38**, 3044 (2013).
13. H. K. Choi, M. S. Ahsan, D. Yoo, I. B. Sohn, Y. C. Noh, J. T. Kim, D. Jung, J. H. Kim, and H. M. Kang, Opt. Laser Technol. **75**, 63 (2015).
14. M. K. Bhuyan, P. K. Velpula, J. P. Colombier, T. Olivier, N. Faure, and R. Stoian, Appl. Phys. Lett. **104**, 021107 (2014).
15. J. Amako, D. Sawaki, and E. Fujii, J. Opt. Soc. Am. B **20**, 2562 (2003).
16. M. Duocastella and C. B. Arnold, Laser Photon. Rev. **6**, 607 (2012).
17. J. Durnin, J. Opt. Soc. Am. A **4**, 651 (1987).
18. Z. Luo, C. Wang, K. Yin, X. Dong, D. Chu, and J. A. Duan, Appl. Phys. A **122**, 1 (2016).